

Scalable GPU-Parallelized FDTD Method for Analysis of Large-Scale Electromagnetic Dosimetry Problems

Jerdvisanop Chakarothai, Kanako Wake, and Soichi Watanabe

Electromagnetic Compatibility Laboratory
National Institute of Information and Communications Technology, Tokyo, 184-8795, Japan
jerd@nict.go.jp, kana@nict.go.jp, wata@nict.go.jp

Abstract — A massively parallel finite-difference time-domain (FDTD) method using a GPU cluster of TSUBAME system has been developed for numerical exposure of a human body to electromagnetic fields. We have also developed and implemented a novel approach for tracing total energy absorbed into a human body in our parallel FDTD code. Our developed FDTD code has shown a strong scalability using 216 nodes and 648 GPUs in total with a high capability to calculate over ten billion cells per second. Whole-body specific absorption rate (SAR) at 200 MHz, as well as its distribution, of a human body with a 0.5 mm resolution with 40000 time steps was found in less than approximately three hours, showing the availability of the method for large-scale EM dosimetry problems.

Index Terms — Exposure assessment, GPU acceleration, parallel FDTD method, scalability, specific absorption rate.

I. INTRODUCTION

Numerical electromagnetic (EM) simulation using an anatomically realistic human model has recently been performed in many engineering fields including medical applications and investigation on EM biological effects [1]. The finite-difference time-domain (FDTD) method [2, 3] is useful for these studies with an application of realistic human model. Recently, many of finely-detailed realistic whole-body human voxel models have been developed by numerous academic groups and research institutes [4-7]. One of the examples is an anatomically realistic human voxel model of a Japanese adult male and female, and children, developed by National Institute of Information and Communications Technology, Japan [5, 6]. These models have a complex shape and structure of internal organs. Computation of the absorbed energy or the specific absorption rate (SAR) in such a detailed model actually requires the use of high-performance computation systems because a large scale of the models actually results in heavy burdens of computation. Specifically, dosimetry of induced electric field inside a human body, relating to stimulation effect by a trigger of

action potential in nervous cells at MHz-band frequencies, requires analyses of a finely-detailed human model with a resolution less than 1 mm [8]. Analysis of such a fine model will consume very large memory and could take prohibitively long calculation time by using a single workstation.

By virtue of the rapid development of computer industry, other types of processing units like Graphics Processing Unit (GPU) and Many Integrated Core (MIC) Architecture have been developed in order to improve the computation efficiency. Calculation algorithm of the FDTD method is seen suitable for such parallel computation since it requires only field information at the adjacent grid point for the communication between computing nodes. Nagaoka et al. [9] used multi-GPU system (3 GPUs/node) for FDTD simulations to cover a small memory size of a single GPU card, and achieved a speedup rate of 1.5 times compared to NEC SX-8R supercomputer. Kim and Park [10] used the overlap communication model in order to increase efficiency of parallelization. Xu et al. [11] used up to 80 NVIDIA Tesla K20 GPUs for FDTD simulations without a boundary and they found a linear scalability with parallel efficiency of higher than 95%.

In this paper, we implement a parallel FDTD algorithm for numerical EM exposure assessment of finely-detailed human model on the TSUBAME GPU cluster at Tokyo Institute of Technology, Japan. Different from previous implementation of parallel FDTD method on a GPU cluster [9], where it used only z-axis decomposition of the model to map the E and H data into each GPU's memory, our implementation apply a 3D/1D hybrid domain decomposition, in which the total analysis domain is divided into small regions along three axes (x , y , and z), and those regions for each node are further divided along one-dimensional axis into sub-regions to be mapped into each GPU in a node. By using this domain decomposition approach, the communication between nodes is kept as less as possible. An approach for tracing the whole-body SAR in time domain is also implemented in Section II. We first investigate performance of the parallel FDTD method on

TSUBAME systems, then discuss the validity of the method and parallel performance results in Section III. In Section IV, an application of the FDTD method to numerical EM exposure assessment of a realistic human model is demonstrated and the conclusion is eventually drawn in Section V.

II. IMPLEMENTATION OF PARALLEL FDTD METHOD ON GPU CLUSTER

GPU has a hierarchical memory structure and it consists of more than 2,000 computing cores (known as CUDA cores), depending on the generation and type of the GPU. In order for a GPU to reach its best performance, we have to consider GPU architecture in the implementation. Here we use an Integrated Development Environment of CUDA, provided by NVIDIA Corp. for GPU programming [12].

In this paper, we adopt the scattered-field formulation of the FDTD method so as to enable arbitrary incident field as a source. The update equations of the scattered-field FDTD method are derived by discretizing the Maxwell's equations, and for an interest reader, the detail of the FDTD formulation can be found in [4].

A. New approach for tracing whole-body SAR in time course

Here we use a new algorithm for determining whole-body average SAR or total absorption energy in a biological body for finding convergence of the FDTD solution. First, assume that we have two identical problem domains but their incident EM fields have a constant phase difference equal to a specific difference of $\Delta\theta$ at every grid point in the analysis domain as shown in Fig. 1, the field solutions for both problem domains will result in the same phase difference of $\Delta\theta$. The FDTD solutions obtained from each analysis domain, applying a single-frequency continuous sinusoidal waveform as incident EM fields, are also represented in the sinusoidal form as follows:

$$X_1(t) = A\sin(\omega t + \theta_1) \text{ for domain } D_1, \quad (1)$$

$$X_2(t) = A\sin(\omega t + \theta_2) \text{ for domain } D_2, \quad (2)$$

where $X_1(t)$ and $X_2(t)$ are the FDTD-calculated quantities; e.g., electric or magnetic fields, at the same location in the problem domain D_1 and D_2 , respectively. A represents magnitude of the field solution which is equal in both analysis domains, θ_1 and θ_2 are the phase of the solutions in D_1 and D_2 , respectively. The phase difference has a known constant value, i.e., $\Delta\theta = \theta_2 - \theta_1$. We can determine the cosine components of the solution by substituting $\Delta\theta$ into (2) and obtain:

$$\begin{aligned} X_2(t) &= A\sin(\omega t + \theta_1 + \Delta\theta) \\ &= AX_1(t)\cos(\Delta\theta) + A\cos(\omega t + \theta_1)\sin(\Delta\theta), \\ A\cos(\omega t + \theta_1) &= \frac{X_2(t) - X_1(t)\cos(\Delta\theta)}{\sin(\Delta\theta)}. \end{aligned} \quad (3)$$

Therefore, a square of the field magnitude A at arbitrary location in the problem domain is eventually found as:

$$\begin{aligned} A^2 &= X_1^2(t) + \frac{[X_2(t) - X_1(t)\cos(\Delta\theta)]^2}{\sin^2(\Delta\theta)} \\ &= \frac{X_1^2(t) + X_2^2(t) - 2X_1(t)X_2(t)\cos(\Delta\theta)}{\sin^2(\Delta\theta)}. \end{aligned} \quad (4)$$

Meanwhile, the specific absorption rate (SAR) at arbitrary location in biological tissues is defined by the following equations:

$$\text{SAR} = \frac{\sigma}{2\rho} |\mathbf{E}|^2 = \frac{\sigma}{2\rho} (E_x^2 + E_y^2 + E_z^2), \quad (5)$$

where σ and ρ are the conductivity and density of the biological tissues. Therefore, Eq. (4) can be used for finding a square of electric field components in (5). The whole-body average SAR is then found by dividing total absorption energy with its weight W ,

$$\text{WBSAR} = \frac{\sum \rho \text{SAR}}{W}. \quad (6)$$

In this way, we can determine whole-body SAR or total energy absorbed into a human body at any instant in time course and decide whether or not the solution reaches convergence in order to terminate the computation. This algorithm can be easily implemented into the conventional FDTD code by calculating an identical problem domain having an incident field of a constant phase difference in parallel.

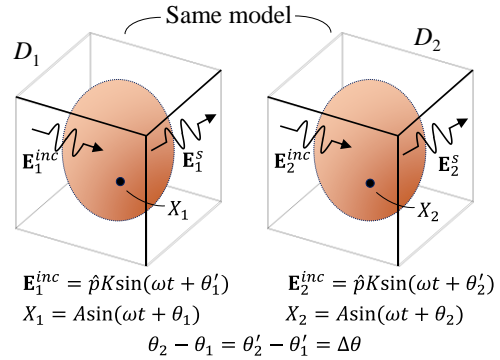


Fig. 1. Concept of an approach for determination of the whole-body average SAR in time course by defining two identical problem domain D_1 and D_2 with an incident field having a constant phase difference of $\Delta\theta = \theta_2' - \theta_1'$. K and A are the magnitude of the incident electric field $\mathbf{E}_{1,2}^{inc}$ and the FDTD-calculated field of the solution, respectively, \hat{p} is the polarization vector.

B. Parallel FDTD implementation on GPU cluster

In order to employ multiple GPUs for the FDTD calculation, we adopt a hybrid 3D/1D domain decomposition as shown in Fig. 2. The whole FDTD analysis region is divided into several regions for each node in a three-dimensional way so as to reduce data size for the communications between nodes. Since each node

contains multiple GPUs, all divided regions are again decomposed into sub-regions in one-dimensional axis, and mapped to each GPU in a node. N_x , N_y , and N_z are number of voxels in x , y , and z axes, respectively. Total number of regions is equal to $M_x \times M_y \times M_z$, where M_x , M_y , and M_z are number of blocks in x , y , and z axes, respectively. Obviously, there are $(N_x/M_x) \times (N_y/M_y) \times (N_z/M_z)$ voxels for each region. Each region is then decomposed in one dimensional way in the z axis in order to be mapped in each GPU memory in an individual node. Size of the region associated to each GPU is equal to $(N_x/M_x) \times (N_y/M_y) \times (N_z/(N_{\text{GPU}}M_z))$ voxels, where N_{GPU} denotes number of GPUs in each node.

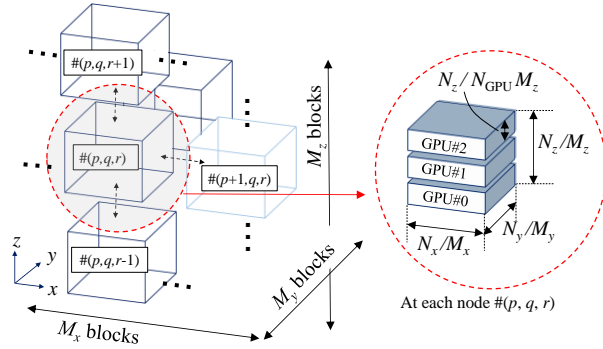


Fig. 2. Hybrid 3D/1D domain decomposition for multi-GPU computation. Total region is divided into M_x , M_y , and M_z blocks along the x , y , and z axes. Each block, corresponding to each computation node in the cluster, has a size of $(N_x/M_x) \times (N_y/M_y) \times (N_z/M_z)$ cells, where N_x , N_y , and N_z are number of voxels in x , y , and z directions. Each block is divided into many sub-regions along z axis and assigned to each GPU in computing nodes. p , q , and r indicate block index in x , y , and z axes, respectively.

Since the FDTD method is based on a finite difference scheme, electric and magnetic fields at a grid point are updated by referring information at the adjacent grid point. At the boundary, since the adjacent grid data resides in another GPU memory, we need to copy the data from one GPU memory to another GPU memory. The process of communications in the GPU cluster consists of three steps: (a) memory copy from GPU to host; (b) MPI send and receive communications; (c) memory copy from host to GPU. The communications between two nodes for electric field data in the GPU cluster are schematically shown in Fig. 3. Since the data in a node is mapped to multiple GPUs and the data in GPU memory does not locate in a consecutive order, so we need to rearrange the data to a consecutive temporary memory in each GPU in order to be copied once to the host memory and then we collect the data from each GPU and copy to the host memory for the boundary data at the left ($-x$) and front ($-y$) direction (see Fig. 3). The boundary data in the ($-z$) direction is arranged in a

consecutive way. Therefore, the consecutive data at the $-z$ boundary can be directly copied from the GPU memory to the host node memory. Internode communications are done by using ‘MPI_send’ and ‘MPI_receive’ command of the MPI (Message Passing Interface). After the communications, the data must be copied back to the GPU memory and mapped to the original location in the memory for each GPU as shown in Fig. 3. The data flow for the magnetic field data and the internode communications are the same but in a reverse direction. It should be noted that the communications between the GPUs inside a node can be done effectively and directly by using the NVIDIA GPUdirect function of ‘cudaMemcpyPeer’ [11].

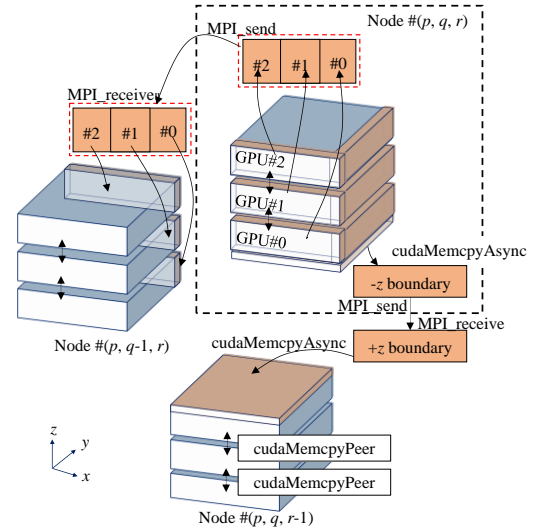


Fig. 3. Communications between nodes for electric field data. The electric field data at the front ($-y$) faces are gathered into one package before sending to another node by ‘MPI_send’ command while the data at the bottom ($-z$) face is retrieved only from the GPU index #0 and sent to the GPU index #2 of another node. Data communications between GPUs inside a node is directly done by the ‘cudaMemcpyPeer’ command. The data communications at the left ($-x$) face is done in the same manner with that of the front face. Data flow of the internode communications for magnetic field are performed in reverse way.

Figure 4 illustrates the program flowchart of the FDTD computation in the GPU cluster. First, in order to perform calculation on a GPU cluster, we need to transfer material data of a human model to GPU memory. The loop of the FDTD calculation is then started with update of the electric field data. It should be noted that some special treatment and calculation; e.g., separate memory allocation, for the field data at the PML boundaries is required. The SAR of each cell is also determined via (6) in this step. It is apparent that the SAR

calculation method proposed in this paper requires that analyses of two identical models with incident fields having phase different are simultaneously performed on the same GPU node. Consequently, memory usage and computation burden are also twice of the original FDTD method. After updating the electric field, the field data at the boundary between GPUs inside a node is directly transferred with the ‘GPUdirect’ function, whereas the boundary data must be packed into one bundle to reduce number and time of communications. The data bundle in the GPU memory is then transferred to the host memory and communicated through MPI functions. Before updating magnetic field, the boundary data is then copied back to the GPU memory and unpacked to the original grid points. After updating magnetic fields and those at the PML boundaries, the inter-GPU and internode communications are performed in the same way with those done for electric field data. The loop is repeated until the whole-body SAR or total absorbed energy reaches convergence and the calculated electric and magnetic fields are finally copied to the host memory.

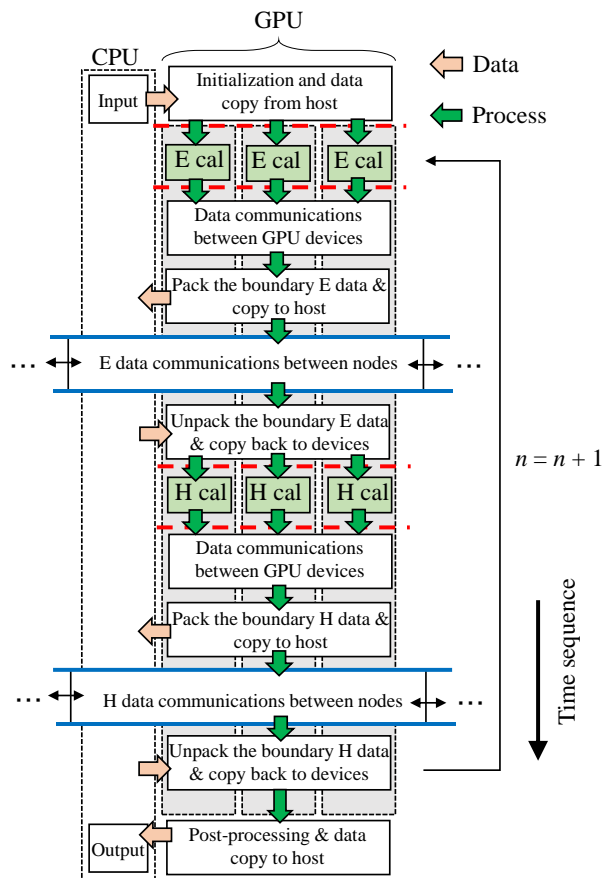


Fig. 4. Illustrative flowchart of the FDTD computation in a computing node. Dash line indicates synchronization between GPU devices (red dotted line) and MPI barrier between nodes (blue solid line).

In order to improve the GPU performance, all three-dimensional field data are allocated as one-dimensional array. Second, the communications between the GPUs inside a node are performed in an asynchronous mode. The asynchronous mode takes advantage of the GPU computational power and PCIe bandwidth. Third, the data for the front and left boundaries (x and y directions as shown in Fig. 3) is not continuous in the GPU memory so that the data packing is required, while the continuous data of the z boundary is directly transferred to the host memory and between nodes.

III. NUMERICAL RESULTS

A. Validity of parallel FDTD code

Most of our simulations are compiled and executed on a large-scale GPU cluster of TSUBAME2.5 system at Tokyo Institute of Technology, Japan. TSUBAME2.5 system has in total 1408 computing nodes. Each node in the GPU cluster is configured with two Intel Westmere-EP X5670 2.93 GHz (Turbo boost 3.2 GHz) of six cores per CPU, and equipped with three NVIDIA Tesla K20x GPUs in each node. There are 1367 computing nodes with 54 GB memory (DDR3-1333) and 41 nodes with 96 GB memory for each. All nodes are connected by two HP QDR InfiniBand. Peak performances of the total system for double- and single-precision floating points are 5.76 PFlops and 17.1 PFlops, respectively, ranking in the 22th fastest supercomputer in Top500 (List of June 2015) [13]. The FDTD code was written using C++ and CUDA using single-precision floating point for calculations which is considered to be sufficient for our dosimetry applications. Number of CUDA threads is fixed to 125 in all numerical experiments. Numerical results obtained from the GPU cluster are also compared to those obtained from an HP workstation equipped with two Intel Xeon CPU E5-2643v3 (3.4 GHz) of six cores (12 threads) per CPU. Main memory of the workstation is 96 GB. Phase difference of incident field of two identical analysis models was set to 90° or $\pi/2$ in all calculations.

Whole-body SAR of a dielectric sphere having a radius of 20 cm, and dielectric properties of $\epsilon_r = 2$ and $\sigma = 0.1$ S/m, illuminated by a plane wave at 200 MHz, is shown in Fig. 5. Strength of incident electric field is 1 V/m. Total size of analysis region was $256 \times 256 \times 256$ cells with a resolution of 2 mm in each axis. Number of calculation time steps was approximately 3000 steps. From Fig. 5, it can be seen that by using a new approach described in Section II, we can trace the whole-body SAR in time course. It is also observed that the whole-body SAR converged within two periods. Therefore, the calculation time can be kept as minimum as possible by using the proposed method. The calculation using GPUs was performed on TSUBAME system using only single node and three GPUs. The whole-body SARs obtained

by CPU (24 parallel threads) and GPU calculations were determined as $8.54 \mu\text{W}/\text{kg}$ and $8.52 \mu\text{W}/\text{kg}$, respectively, showing good agreement of that obtained by analytic Mie's solution of $8.42 \mu\text{W}/\text{kg}$. Errors between the Mie's result and the FDTD method were about 1.38% and 1.12% for the CPU and GPU computations, respectively, demonstrating the validity of the method. Figure 6 shows the SAR distribution of the sphere obtained from each method. It is shown that the SAR distributions of the sphere obtained by the CPU and GPUs are in good agreement with the Mie's solution.

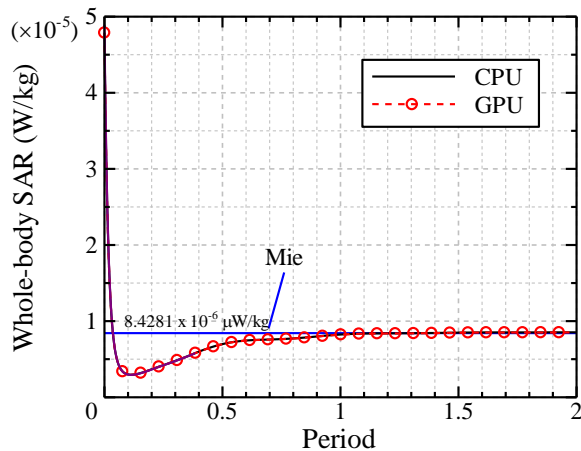


Fig. 5. Whole-body SAR of a dielectric sphere in time course, calculated by a workstation (24 parallel threads) and three GPUs (single node) on TSUBAME system.

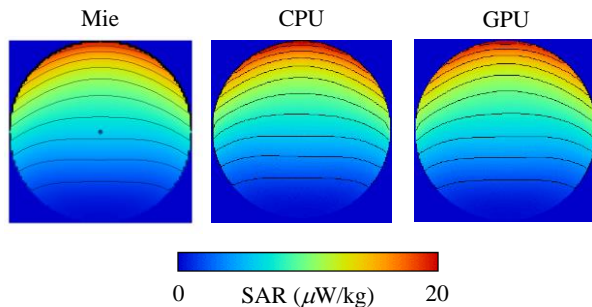


Fig. 6. SAR distribution of a dielectric sphere illuminated by a plane wave at 200 MHz, by the Mie's solution, and those obtained from the CPU and GPU computations.

B. Scalability and parallelization efficiency

We use a hybrid 3D/1D domain decomposition and the parallel FDTD method described in the previous section for an analysis of a dielectric sphere. In order to demonstrate a scalability of a large-scale EM simulation,

sizes of analysis model of 256^3 , 512^3 , and 1024^3 voxels with a resolution of 2 mm, 1 mm, and 0.5 mm, respectively, were used in the analyses. Number of time steps was 1000 steps in all simulations. Analysis model is a dielectric sphere illuminated with a plane wave at 200 MHz, same with that described in previous subsection.

Figure 7 shows scalability of the computation using multiple computing nodes of TSUBAME system. Vertical axis shows a number of cells divided by calculation time per a time step, indicating how much Yee's cells we can manipulate within a second. The ideal curve was calculated from the result of the 256^3 model calculated using three GPUs; i.e., the ideal number of cells/second N^{ideal} is determined as:

$$N^{\text{ideal}} = \frac{N_{\text{GPU}}}{3} \times N^{3\text{GPUs}}, \quad (7)$$

where $N^{3\text{GPUs}}$ is a number of cells calculated in a second when using three GPUs for the 256^3 model. Horizontal axis indicates a number of GPUs used in the simulations. The black dash line shows the ideal scalability. Our parallel FDTD method shows a strong scalability for a problem domain even when an analysis size grows up to 1024^3 cells. Highest performance using 648 GPUs in parallel was achieved at more than 12 billion cells per second. To the extent of the authors' knowledge, this result is the highest performance achieved by using a GPU cluster for the FDTD method. Table 1 shows the parallelization efficiency of the method varied by number of GPUs used in the simulation. The efficiency of parallelization is determined from a ratio of the real time used in the simulation and the expected time used for ideal parallelization. When number of GPUs is equal to three, there is no field data communications between nodes. The only existing communications is occurred between GPUs in a single computing node, which is performed by using fast GPUdirect technology provided by NVIDIA Corp [12]. The parallelization efficiency decreases as number of GPUs increases due to increase in data communications between nodes. Efficiency achieved by using 648 GPUs in parallel was about 57.1%. Speedup ratios using 180 GPUs and 648 GPUs in parallel were about 91 times and 290 times, respectively, compared to the calculation time used by the 24-cores-in-parallel workstation for the model size of 512^3 cells and 1024^3 cells. It should be noted that the FDTD method used in our simulations requires two identical models to be analyzed at the same time, and therefore computational burden is almost twice of the original FDTD method. Number of time steps can be, however, kept as minimum as possible and the calculation is terminated as soon as the whole-body SAR reaches its convergence in time domain.

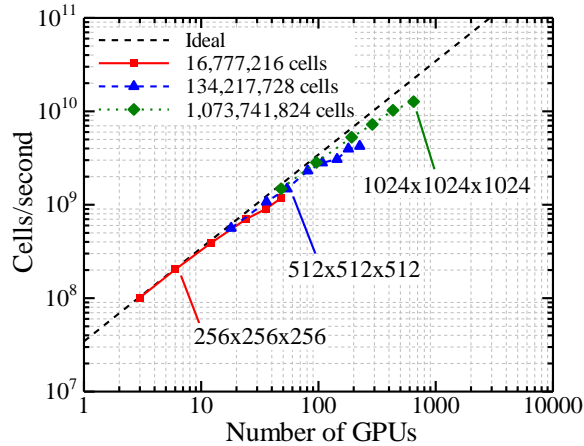


Fig. 7. Scalability for three problem sizes $N = 256^3$, 512^3 , and 1024^3 on TSUBAME system at Tokyo Institute of Technology, Japan.

Table 1: Number of calculated cells per second and parallelization efficiency for various calculated conditions

Number of GPUs	Used Time Per Step (s)	Number of Cells Per Time Step	Efficiency
Model Size : $256 \times 256 \times 256$			
3	0.1629	102,964,265	100.0%
6	0.0827	202,815,601	98.4%
12	0.0433	387,051,310	94.0%
24	0.0240	698,846,918	84.8%
48	0.0143	1,176,439,090	71.4%
Model Size : $512 \times 512 \times 512$			
18	0.2389	561,866,603	91.0%
36	0.1250	1,074,102,769	86.9%
54	0.0905	1,483,221,863	80.0%
108	0.0477	2,813,593,720	75.9%
180	0.0338	3,965,555,632	64.2%
Model size : $1024 \times 1024 \times 1024$			
48	0.7240	1,482,935,432	90.0%
96	0.3790	2,833,282,897	86.0%
192	0.2052	5,271,676,808	80.0%
432	0.1054	10,257,114,978	69.2%
648	0.0859	12,694,231,253	57.1%

IV. APPLICATION TO DOSIMETRY

Here we employ our parallel FDTD method to a practical problem of EM exposure assessment of a human body. We use a Japanese male model developed by National Institute of Information and Communications Technology, Japan [5]. The model is composed of 51 different tissues and organs with an original resolution of 2 mm. Height and weight of the model were 173 cm and 64 kg, respectively. The permittivity and conductivity of biological tissues are extracted from the Gabriel's data [14]. Figure 8 shows analysis model of a realistic human model, irradiated to an EM plane wave at 200 MHz. The

propagation direction of the z -polarized incident plane wave was along $+x$ direction. Total sizes of analysis domain are $190 \times 350 \times 896$, $350 \times 670 \times 1767$, and $670 \times 1310 \times 3498$ cells for a model resolution of 2 mm, 1 mm, and 0.5 mm respectively. Maximum number of time step was 10000, 20000, and 40000 steps for the 2 mm, 1 mm, and 0.5 mm models, respectively.

Figure 9 indicates the whole-body average SAR of human body in time course, excited by a plane wave at 200 MHz. It is obvious that the WBSAR converges to a constant value within five periods. The WBSAR of the human with 2 mm, 1 mm, and 0.5 mm resolutions was calculated as $13.6 \mu\text{W}/\text{kg}$, $13.9 \mu\text{W}/\text{kg}$, and $14.0 \mu\text{W}/\text{kg}$, respectively, for an incident electric field strength of 1 V/m. Calculation time in finding the whole-body SAR for 2 mm resolution was approximately 227 minutes using a 24-core (3.5 GHz) workstation with OpenMP, while it was only 13 minutes when using 24 GPUs which is about 17 times faster. The dosimetry analysis of the whole human model with a 1 mm resolution takes about 85 minutes by using 54 GPUs in parallel, which was approximately 47 times faster than computation by our 24-core workstation. The calculation time for the 0.5 mm model with 40000 time steps was less than 3 hours (175 minutes). Figure 10 illustrates the SAR distribution calculated by using the GPU cluster with 24, 54, and 432 GPUs. The SAR distributions obtained by either the workstation or the GPU cluster of TSUBAME are in good agreement each other, showing availability and efficiency of our parallel FDTD code in use with the GPU cluster. From our results, speedup ratio can be achieved at a rate of more than a thousand times faster than using a single-core workstation, depending on number of GPUs used in analysis.

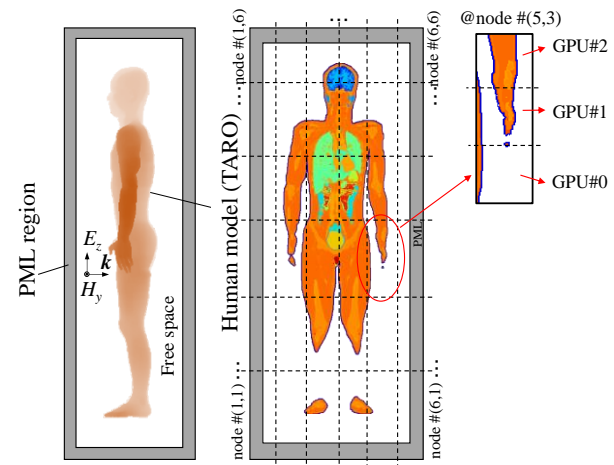


Fig. 8. Analysis model of EM exposure assessment of a realistic human model and the model decomposition into 6×6 blocks in yz -plane. Each block corresponds to a computation node with three GPUs inside.

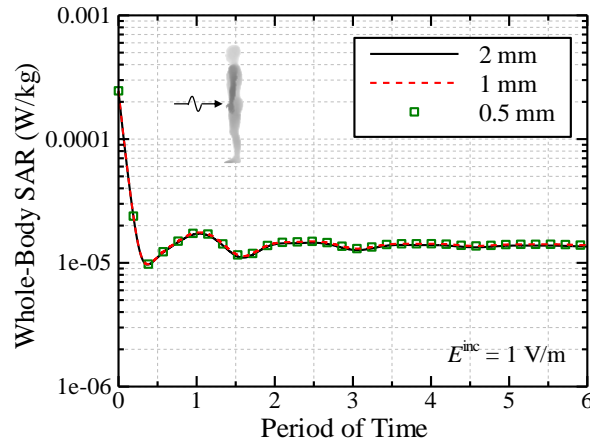


Fig. 9. Whole-body SAR with respect to period of actual time for 2 mm, 1 mm, and 0.5 mm human models.

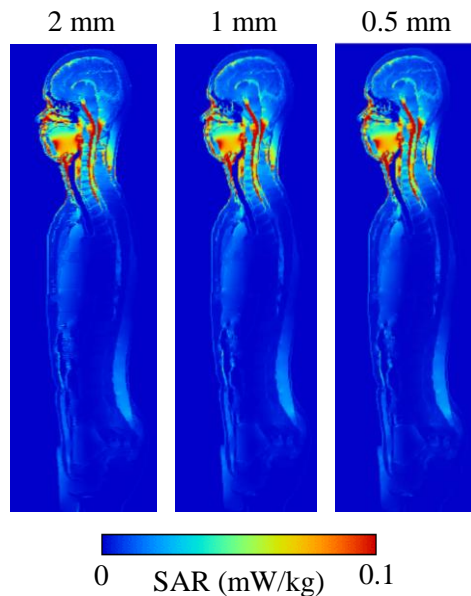


Fig. 10. SAR distribution in the human models.

V. CONCLUSION

A scalable and parallel finite-difference time-domain method for a large-scale electromagnetic simulation of human exposures using the GPU cluster of TSUBAME system has been developed. A novel approach for tracing the convergence of the whole-body SAR in a time course has also been adapted in our FDTD-GPU code. Validity of the method was demonstrated by comparing with the analytical Mie's results of the dielectric sphere. Strong scalability with parallelization efficiency of 57% has been found for an analysis model size up to 1024^3 grid cells using 216 nodes and 648 GPUs in total. High performance of the FDTD calculation with more than 12 billion cells per second can be achieved using in total 648 GPUs in parallel. Finally, the numerical exposure of

a human body having a resolution of 0.5 mm and a model size of $670 \times 1310 \times 3498$ cells, irradiated by EM plane wave at 200 MHz, has been performed and the simulation was terminated in about 175 minutes for 40000 time steps using 144 nodes with 432 GPUs of TSUBAME system. A high computation performance of our parallel FDTD method for large-scale EM dosimetry has been demonstrated and achieved by using the GPU cluster of TSUBAME system.

The analysis of a signal triggered in human nervous system due to EM exposures at MHz-band frequencies will be done by using the TSUBAME GPU cluster in the future.

ACKNOWLEDGMENT

This study was financially supported by the Ministry of Internal Affairs and Communications, Japan. Most of numerical results in this study were carried out using a high-performance GPU cluster of TSUBAME system at Tokyo Institute of Technology, Tokyo.

REFERENCES

- [1] D. M. Sullivan, D. T. Borup, and O. P. Gandhi, "Use of the finite-difference time-domain method in calculating EM absorption in human tissues," *IEEE Trans. Biomedical Engineering*, vol. BME-34, no. 2, pp. 148-157, Feb. 1987.
- [2] K. S. Yee, "Numerical solution of initial boundary value problems involving Maxwell's equations in isotropic media," *IEEE Trans. Antennas Propag.*, vol. 14, no. 4, pp. 302-307, 1966.
- [3] K. S. Kunz and R. J. Luebbers, *The Finite Difference Time Domain Method for Electromagnetics*, CRC Press, May 3, 1993.
- [4] P. J. Dimbylow, "FDTD calculations of the whole-body averaged SAR in an anatomically realistic voxel model of the human body from 1 MHz to 1 GHz," *Phys. Med. Biol.*, vol. 42, pp. 479-490, 1997.
- [5] T. Nagaoka, S. Watanabe, K. Sakurai, E. Kunieda, S. Watanabe, M. Taki, and Y. Yamanaka, "Development of realistic high-resolution whole-body voxel models of Japanese adult and females of average height and weight, and application of models to radio-frequency electromagnetic field dosimetry," *Phys. Med. Biol.*, vol. 49, pp. 1-15, 2004.
- [6] T. Nagaoka, E. Kunieda, and S. Watanabe, "Proportion corrected scaled voxel models for Japanese children and their application to the numerical dosimetry of specific absorption rate for frequencies from 30 MHz to 3 GHz," *Phys. Med. Biol.*, vol. 53, pp. 6695-6711, 2008.
- [7] A. Christ, W. Kainz, E. G. Hahn, K. Honegger, M. Zefferer, E. Neufeld, W. Rascher, R. Janka, W. Bautz, J. Chen, B. Kiefer, P. Schmitt, H.-P.

Hollenbach, J. Shen, M. Oberle, D. Szczerba, A. Kam, J. W. Guag, and N. Kuster, "The virtual family – development of surface-based anatomical models of two adults and two children for dosimetric simulations," *Phys. Med. Biol.*, vol. 55, pp. N23-N38, 2010.

- [8] I. Laakso, H. Matsumoto, A. Hirata, Y. Terao, R. Hanajima, and Y. Ugawa, "Multi-scale simulations predict responses to non-invasive nerve root stimulation," *J. Neural Eng.*, vol. 11, pp. 1-9, 2014.
- [9] T. Nagaoka and S. Watanabe, "Accelerating three-dimensional FDTD calculations on GPU clusters for electromagnetic field simulation," in *Proceedings of the Annual International Conference of the IEEE Engineering in Medicine and Biology Society (EMBC'12)*, pp. 5691-5694, 2012.
- [10] K. H. Kim and Q. H. Park, "Overlapping computation and communication of three-dimensional FDTD on a GPU cluster," *Computer Physics Communications*, vol. 183, pp. 2364-2369, 2012.
- [11] L. Xu, Y. Xu, R. Jiang, and D. Zhang, "Implementation and optimization of three-dimensional UPML-FDTD algorithm on GPU cluster," *Computer Engineering & Science*, vol. 35, p. 160, 2013.
- [12] NVIDIA, NVIDIA CUDA programming guide version 4.0, NVIDIA Corporation, 2011.
- [13] TOP500 supercomputer, <http://www.top500.org>
- [14] C. Gabriel, "Compilation of the dielectric properties of body tissues at RF and microwave frequencies," *Brooks AFB, San Antonio, TX, Brooks Air Force Tech. Rep.*, AL/OE-TR-1996-0037, 1996.



Jerdvisanop Chakarothai receives his B.E. degree in Electrical and Electronic Engineering from Akita University, Akita, Japan, in 2003 and his M.E. and D.E. degrees from Tohoku University, Sendai, Japan, in 2005 and 2010, respectively, both in Electrical and Communication Engineering.

He was a Research Associate at Tohoku University from 2010, prior to joining the Nagoya Institute of Technology, Nagoya, Japan, in 2011. He was a Research Associate at Tokyo Metropolitan University in 2013. He is currently with the National Institute of Information and Communications Technology, Tokyo, Japan. His research interests include computational bio-electromagnetics and electromagnetic compatibility. He received the 2014 Young Scientist Award from the International Scientific Radio Union.



Kanako Wake received her B.E., M.E. and D.E. degrees in Electrical Engineering from Tokyo Metropolitan University, Tokyo, Japan, in 1995, 1997, and 2000, respectively.

She is currently with the National Institute of Information and Communications Technology, Tokyo, Japan, where she is involved in research on biomedical electromagnetic compatibility.



Soichi Watanabe received the B.E., M.E. and D.E. degrees in Electrical Engineering from Tokyo Metropolitan University, Tokyo, Japan, in 1991, 1993, and 1996, respectively.

He is currently with the National Institute of Information and Communications Technology, Tokyo. His main research interest includes biomedical electromagnetic compatibility.

Watanabe is a Member of IEEE and the Bio-electromagnetics Society. From 2004 to 2012, he is a Member of the Main Commission of ICNIRP from 2012. He received the 1996 Young Scientist Award from the International Scientific Radio Union, the 1997 Best Paper Award from IEICE, and the 2004 Best Paper Award (The Roberts Prize) of Physics in Medicine and Biology.